Synthesis and Separation Performance of SSZ-13 Zeolite Membranes on Tubular Supports

Halil Kalipcilar, Travis C. Bowen, Richard D. Noble, and John L. Falconer*

Department of Chemical Engineering, University of Colorado, Boulder, Colorado 80309-0424

Received March 7, 2002. Revised Manuscript Received June 5, 2002

SSZ-13 zeolite membranes were synthesized on the inside surface of porous stainless steel tubes. In parallel with zeolite pores, the membranes had nonzeolite pores that were larger than the 0.38-nm zeolite pore diameter, but single-gas permeances of H_2, N_2, CH_4, and n-C_4H_{10} decreased with increasing kinetic diameter at 298 K. The CO_2/CH_4, H_2/CH_4 and H_2/n-C_4H_{10} ideal selectivities were 11, 9.0, and 63, respectively, at 298 K, and the separation selectivities for the mixtures of the same gas pairs were 12, 8.2, and 5.7 at 298 K. The SSZ-13 membranes selectively removed H_2O from HNO_3/H_2O liquid mixtures by pervaporation to break the azeotrope at 69.5 wt % HNO_3. The permeate concentration was 38.3% HNO_3, and the total flux was 0.12 kg/m^2·h at 298 K.

Introduction

Zeolite membranes have the potential to efficiently separate hydrocarbon vapor and light-gas mixtures containing small molecules that weakly adsorb because of the nanoporous structure and adsorption properties of zeolites. Most studies have focused on MFI zeolite membranes,[1−4] which have an XRD pore size of approximately 0.54 nm and are not suitable for separating light gases unless the MFI crystals on the membrane surface are oriented in a certain direction.[5,6] Therefore, zeolite membranes with smaller pore sizes would be more practical for light-gas separation.

A few studies have reported the preparation of membranes composed of small-pore zeolites, such as analcime,[7] zeolite A,[8,9] SAPO-34 (CHA structure),[10,11] ETS-4,[12] and MAPO-39 (ATN structure).[13] Zeolite A membranes have been used to separate H_2/N_2, O_2/n-C_4H_{10}, and H_2/n-C_4H_{10} mixtures.[8,9] The respective selectivities were approximately 4.4, 2, and 4.6 at 300 K. Although zeolite A membranes were effective at separating water/alcohol mixtures by pervaporation,[14] their gas separation selectivities were close to the Knudsen selectivities. In contrast, SAPO-34 membranes separated CO_2/CH_4, CO_2/N_2, and H_2/CH_4 mixtures with selectivities of approximately 36, 16, and 7.5, respectively, at 298 K.[10,11] Guan et al.[12] prepared ETS-4 membranes that were selective for N_2 over O_2, CH_4, and CO_2. The N_2/CH_4 and N_2/CO_2 selectivities were approximately 5 and 4, respectively, at 308 K.

The permeation measurements for SAPO-34 membranes[10,11,15] show that zeolites with the chabazite structure are good candidates for light-gas separations. Several membranes with the chabazite structure have been reported. Membranes consisting of a mixture of chabazite, mordenite, and ZSM-5 were synthesized on α-alumina supports and found to separate propanol/water vapor mixtures with a separation factor of 71.[16,17] However, these membranes are not suitable for separating small molecules because of their wide pore size distribution and the larger pore sizes of mordenite and MFI crystals, which constituted approximately 75% of the membrane.[16] Lee and Dutta[18] prepared pure, free-standing chabazite films. These films had weak mechanical stability and therefore were not used for separation.

Zeolite membranes have been used to separate water/organic,[19−22] organic/water,[23−29] organic/organic,[30−33]

* To whom correspondence should be addressed. Phone: 303-492-8005. Fax: 303-492-4341. E-mail: john.falconer@colorado.edu.

(1) Funke, H. H.; Kovalchick, M. G.; Falconer, J. L.; Noble, R. D. *Ind. Eng. Chem. Res.* **1996**, *35*, 1575.
(2) Kusakabe, K.; Yoneshige, S.; Murata, A.; Morooka, S. *J. Membr. Sci.* **1996**, *116*, 39.
(3) Yan, Y.; Davis, M. E.; Gavalas, G. R. *Ind. Eng. Chem. Res.* **1995**, *34*, 1652.
(4) Tuan, V. A.; Falconer, J. L.; Noble, R. D. *Ind. Eng. Chem. Res.* **1999**, *38*, 8, 3635.
(5) Lovallo, M. C.; Tsapatsis, M. *AIChE J.* **1996**, *42*, 3020.
(6) Lovallo, M. C.; Gouzinis, A.; Tsapatsis, M. *AIChE J.* **1998**, *44*, 1903.
(7) Mimura, H.; Tezuka, T.; Akiba, K. J. *Nucl. Sci. Technol.* **1995**, *32*, 1250.
(8) Aoki, K.; Kusakabe, K.; Morooka, S. J. *Membr. Sci.* **1998**, *141*, 197.
(9) Aoki, K.; Kusakabe, K.; Morooka, S. *Ind. Eng. Chem. Res.* **2000**, *39*, 2245.
(10) Poshusta, J. C.; Tuan, V. A.; Pape, E. A.; Noble, R. D.; Falconer, J. L. *AIChE J.* **2000**, *46*, 779.
(11) Poshusta, J. C.; Noble, R. D.; Falconer, J. L. *J. Membr. Sci.* **2001**, *186*, 25.
(12) Guan, G.; Kusakabe, K.; Morooka, S. *Microporous Mesoporous Mater.* **2001**, 50, 109.
(13) Kriel-Washmon, L.; Balkus Jr., K. J. *Microporous Mesoporous Mater.* **2001**, *38*, 107.
(14) Okamoto, K.; Kita, H.; Horii, K.; Tanaka, K.; Kondo, M. *Ind. Eng. Chem. Res.* **2001**, *40*, 163.
(15) Poshusta, J. C.; Noble, R. D.; Falconer, J. L. *J. Membr. Sci.* **2001**, *186*, 25.
(16) Salomon, M. A.; Coronas, J.; Menendez, M.; Santamaria, J. *J. Chem. Soc., Chem. Commun.* **1998**, 125.
(17) Piera, E.; Salomon, M. A.; Coronas, J.; Menendez, M.; Santamaria, J. *J. Membr. Sci.* **1998**, *149*, 99.
(18) Lee, H.; Dutta, P. K. *Microporous Mesoporous Mater.* **2000**, *38*, 151.
(19) Kita, H.; Horii, K.; Ohtoshi, Y.; Tanaka, K.; Okamoto, K. I. *J. Mater. Sci. Lett.* **1995**, *14*, 206.
(20) Kondo, M.; Komori, M.; Kita, H.; Okamoto, K. I. *J. Membr. Sci.* **1997**, *133*, 133.
(21) Shah, D.; Kissick, K.; Ghorpade, A.; Hannah, R.; Bhattacharvya, D. *J. Membr. Sci.* **2000**, *179*, 185.
(22) Kita, H.; Asamura, H.; Tanaka, K.; Okamoto, K. I. *ACS Symp. Ser.* **2000**, *744*, 330.
(23) Nomura, M.; Yamaguchi, T.; Nakao, S. I. *J. Membr. Sci.* **1998**, *144*, 161.

10.1021/cm020248i CCC: $22.00
Published on Web 07/10/2002

and weak acid/water solutions [34,35] with high separation factors by pervaporation. Sano et al.[35] observed that silicalite membranes selectively permeated acetic acid with a separation factor of 2.6 for a 5 vol % acetic acid/water solution at 303 K, but these membranes did not exhibit selectivity for a 60 vol % acetic acid/water solution. Li et al.[35] measured separation factors as high as 14 for acetic acid removal from 5 wt % acetic acid/water mixtures using Ge−ZSM-5 membranes at 363 K. However, to our knowledge, no studies have been performed using zeolite membranes to separate aqueous strong acid solutions such as nitric acid. Separating concentrated strong acid solutions requires hydrophilic, acid-resistant membranes. The hydrophilicity of zeolites increases with Al content in the framework,[36] whereas the acid resistance simultaneously decreases because strong acids leach Al from the zeolite.[37−39]

The present paper reports the synthesis and characterization of SSZ-13 zeolite membranes. The SSZ-13 zeolite has the chabazite (CHA) structure and a Si/Al ratio of 14. Its framework contains a tridimensional pore system made up of 0.38-nm, eight-membered oxygen rings.[40] Single-gas permeances and light-gas separations were used for membrane characterization. Aqueous nitric acid at the azeotropic concentration (69.5 wt % HNO_3) was dehydrated by pervaporation. The SSZ-13 zeolite was chosen because its pore size is comparable to the size of light gases and between the kinetic diameters of HNO_3 (0.39 nm) and H_2O (0.27 nm). In addition, SSZ-13 is expected to be reasonably stable in acid but not highly hydrophilic because of its high Si/Al ratio.

Experimental Methods

Membrane Preparation. The membranes were hydrothermally synthesized onto the inside surface of two types of porous, stainless steel tubes. One type (Pall Corporation) had a 44% porosity and 4-μm nominal pore diameter. The porous section of this support was 29-mm long with an inside diameter of 8.6 mm and an outside diameter of 10 mm. The other type (Mott Corporation) had a 27% porosity and a 0.5-μm nominal pore diameter. This type had a 25-mm-long porous section with 6.5-mm i.d. and 9.5-mm o.d.

Table 1. SSZ-13 Membranes on Porous Stainless Steel Tubes

membrane	support	seeding	number of layers
M1	Pall	yes	4
M2	Pall	yes	4
M3	Pall	yes	4
M4	Mott	yes	5
M5	Mott	yes	5
M6	Mott	yes	5
M7	Pall	no	5
M8	Pall	no	5

Prior to membrane preparation, the inner surface of the support was covered by SSZ-13 seed crystals, which were synthesized from a gel with a molar composition of 10 Na_2O: 2.5 Al_2O_3:100 SiO_2:4400 H_2O:20 TMAdaOH. The gel was prepared as described by Robson.[40] The reactants were Cab-o-sil amorphous silica, $Al(OH)_3$, NaOH, and 0.7 M TMAdaOH solution. The solution of the organic template, *N*,*N*,*N*-trimethyl-1-adamantammonium hydroxide (TMAdaOH), was prepared by a procedure provided by Chevron Corporation. Initially, TMAdaI was prepared by mixing 1-adamantanamine (97%, Aldrich), $KHCO_3$, and methyl iodide in methanol. After the mixture had been stirred for 4 days at room temperature, the solvent was removed with a rotary evaporator. The product was dissolved in chloroform, and the resulting solution stirred for 1.5 h. The mixture was then filtered, and the solvent in the remaining clear solution was removed with a rotary evaporator. The product was slowly dissolved in methanol at reflux temperature and recrystallized. Small, white TMAdaI flakes were converted to TMAdaOH by ion exchange by mixing them with Dowex 550A OH^- resin (Aldrich).

The synthesis of SSZ-13 crystals was carried out in an autoclave at 433 K for 5 days, and the crystals were washed with distilled water and dried overnight at 373 K under vacuum. Approximately 0.1 g of crystals was suspended in 10 mL of distilled water, and this suspension was poured into the tubular support, which had been wrapped with Teflon tape on the bottom. Then, the top was wrapped with Teflon tape, and the support was shaken for 10 min. The seed/water suspension was poured out and the support was dried at 373 K under vacuum for 30 min. This process was repeated twice to deposit crystals on the inside of the membrane tube.

For membrane synthesis, the outer surface and bottom of the support were wrapped with Teflon tape, and the bottom was plugged with a Teflon cap. The support was filled with the synthesis gel, and the top of the support was wrapped with Teflon tape and plugged with a Teflon cap. The gel composition and the synthesis conditions were the same as those for the seed crystal synthesis. Four or five synthesis layers were required to obtain a membrane that was impermeable to N_2 after drying at 373 K under vacuum. The N_2 permeation was tested with a 138-kPa pressure drop at room temperature. The membrane was calcined in air at 753 K for 15 h using heating and cooling rates of 0.01 and 0.03 K/s, respectively, to remove the template from the zeolite framework. Table 1 lists the membranes with the numbers of layers and types of supports.

A membrane surface and the powder collected from the bottom of the membrane were analyzed by X-ray diffraction using Cu Kα radiation (Scintag PAD-V instrument). A membrane was broken and examined by SEM (IS1 SX-30 instrument). The resistance of the SSZ-13 structure to HNO_3 was determined by placing approximately 0.2 g of the SSZ-13 powder in 25 cm^3 of 69.5 wt % HNO_3 for 4−5 days at room temperature. The concentration of Al dissolved in the HNO_3 was measured by inductively coupled plasma atomic emission spectroscopy (ICP-AES). The Si/Al ratio of a membrane was measured with energy-dispersive X-ray (EDX) spectroscopy.

Separating Light-Gas Mixtures. Single-gas permeances of H_2, N_2, CO_2, CH_4, *n*-C_4H_{10}, and *i*-C_4H_{10} were measured in a dead-end membrane module at temperatures between 298 and

(24) Sano, T.; Hasegawa, M.; Kawakami, Y.; Kiyozumi, Y.; Yanagishita, H.; Kitamoto, D.; Mizukami, F. *Stud. Surf. Sci. Catal.* **1994**, *84*, 1175.
(25) Liu, Q.; Noble, R. D.; Falconer, J. L.; Funke, H. H. *J. Membr. Sci.* **1996**, *117*, 163.
(26) Smetana, J. F.; Falconer, J. L.; Noble, R. D. *J. Membr. Sci.* **1996**, *114*, 127.
(27) Li, S.; Tuan, V. A.; Noble, R. D.; Falconer, J. L. *AIChE J.* **2002**, *48*, 269.
(28) Tuan, V. A.; Li, S.; Falconer, J. L.; Noble, R. D. *J. Membr. Sci.* **2002**, *196*, 111.
(29) Lin, X.; Kita, H.; Okamoto, K. I. *Ind. Eng. Chem. Res.* **2001**, *40*, 4069.
(30) Kita, H.; Inoue, T.; Asamura, H.; Tanaka, K.; Okamoto, K. I. *Chem. Commun.* **1997**, 45.
(31) Li, S.; Tuan, V. A.; Falconer, J. L.; Noble, R. D. *Chem. Mater.* **2001**, *13*, 1865.
(32) Wegner, K.; Dong, J. H.; Lin, Y. S. *J. Membr. Sci.* **1999**, *158*, 17.
(33) Sano, T.; Hasegawa, M.; Kawakami, Y.; Yanagishita, H. *J. Membr. Sci.* **1995**, *107*, 193.
(34) Sano, T.; Ejiri, S.; Yamada, K.; Kawakami, Y.; Yanagishita, H. *J. Membr. Sci.* **1997**, *123*, 225.
(35) Li, S.; Tuan, V. A.; Noble, R. D.; Falconer, J. L. *Ind. Eng. Chem. Res.* **2001**, *40*, 6165.
(36) Szostak, R. *Molecular Sieves, Principles of Synthesis and Identification*; Van Nostrand Reinhold: New York, 1989; p 313.
(37) Muller, M.; Harvey, G.; Prins, R. *Microporous Mesoporous Mater.* **2000**, *34*, 135.
(38) Giudici, R.; Kouwenhoven, H. W.; Prins, R. *Appl. Catal. A* **2000**, *203*, 101.
(39) Lee, E. F. T.; Rees, L. V. C. *J. Chem. Soc., Faraday Trans. 1* **1987**, *83*, 1531.
(40) Robson, H. *Microporous Mesoporous Mater.* **1998**, *22*, 551.

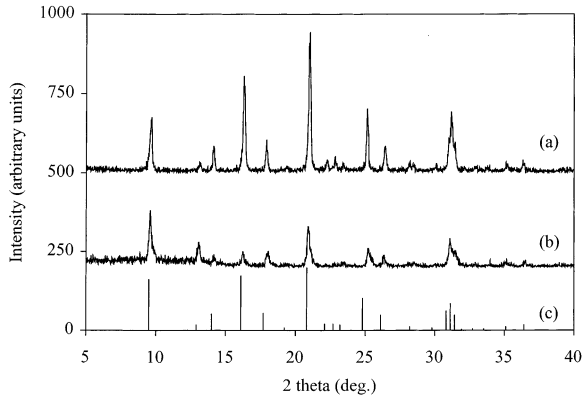

Figure 1. XRD patterns of (a) powder collected during membrane preparation, (b) a SSZ-13 membrane on a porous stainless steel tube (Mott Corp.), and (c) SSZ-13 crystals from ref 40.

473 K. The pressure difference across the membrane was 138 kPa, and the permeate pressure was 85 kPa. Ideal selectivity is defined as the ratio of single-gas permeances.

Fifty/fifty mixtures of light gases were separated from 298 to 473 K in a flow system with a feed flow rate of 40 cm^3/min. The permeate pressure was 85 kPa, and the transmembrane pressure gradient was 138 kPa. Permeate, retentate, and feed concentrations were measured with an on-line GC (HP 5890). Log−mean partial pressure differences were used to calculate the permeances. Separation selectivity is defined as the ratio of permeances.

HNO_3/Water Separation. Water was removed from HNO_3 at the azeotrope concentration using a pervaporation apparatus equipped with a 304-L stainless steel module and a Teflon diaphragm pump that circulated the liquid feed mixture to reduce concentration polarization. Viton O-rings sealed the membrane in the module. Heating tape heated the feed, and the temperature was measured with a thermocouple in the module. The feed volume was 21.5 cm^3, and the flow rate was 2.2 cm^3/s. A mechanical vacuum pump evacuated the permeate side of the membrane to approximately 0.2 kPa. For steady-state measurements, the vacuum pump was used for 2−3 h after the feed mixture had been added. Then, the valve to the pump was closed, and a permeate sample was collected in a liquid-nitrogen cold trap for about 1 h. The permeate pressure remained below 0.4 kPa during sample collection. The sample was weighed to determine the total flux and titrated with 0.02 M NaOH using bromthymol blue indicator to measure the HNO_3 concentration. Feed samples were also titrated to check the feed concentration for each permeate sample collection.

Results and Discussion

Membrane Morphology. A membrane (M6) with five synthesis layers was broken after gas permeation experiments and analyzed by XRD and SEM. The XRD patterns in Figure 1 show that the membrane layer and the powder formed in the synthesis gel have the SSZ-13 structure.[40] The high intensities and the low baselines indicate high purity. The peaks obtained from the membrane layer are weaker than those from the powder because of the small amount of zeolite in the membrane.

The SEM image of the membrane surface shows an SSZ-13 layer (Figure 2a) that consists of spherical particles. The particles, which were 10−20 μm in diameter, are agglomerates of prismatic SSZ-13 crystals, as shown in Figure 2b. The SEM image of the membrane cross section (Figure 2c) shows that the SSZ-13 layer is not uniform and has a thickness of 10−40 μm.

Table 2. Ideal Selectivities for SSZ-13 Membranes

	298 K			473 K			Knudsen
	M1	M3	M5	M1	M3	M5	selectivity
H_2/N_2	5.0	4.0	4.0	4.7	3.8	4.3	3.8
H_2/CH_4	9.0	4.8	5.8	5.1	3.5	3.7	2.8
$H_2/i\text{-}C_4H_{10}$	15	8.4	11	9.9	5.5	7.1	5.4
CO_2/H_2	1.2	1.3	1.6	0.45	0.38	0.34	0.21
CO_2/N_2	5.9	5.0	6.2	2.1	1.4	1.4	0.80
CO_2/CH_4	11	6.2	9.0	2.3	1.3	1.2	0.60

Single-Gas Permeation and Adsorption Effects. Figures 3 and 4 show the single-gas permeances as a function of kinetic diameter at 298 and 473 K. Hydrogen, CO_2, and N_2 are smaller than the zeolite pores. The permeation of $i\text{-}C_4H_{10}$, which is significantly larger than the SSZ-13 pores, indicates that the membranes have nonzeolite pores larger than the 0.38-nm SSZ-13 pore diameter.

The ideal selectivities for all membranes are significantly higher than the Knudsen selectivities at both 298 and 473 K, as shown in Table 2. Membranes had similar ideal selectivities for gas pairs in which both gases fit into the zeolite pores. The ideal selectivities were considerably different for the pairs with one gas larger than the pore size. The differences in ideal selectivities can be ascribed to the differences in the number and size distribution of the nonzeolite pores in the membranes.

As shown in Figures 3 and 4, most permeances decreased with increasing kinetic diameter. However, CO_2 permeated faster than H_2 at 298 K, and CH_4 permeated faster than N_2 at 473 K, although CO_2 is larger than H_2 and CH_4 is larger than N_2. The larger molecules can permeate faster than smaller molecules if they adsorb more strongly.[13−16] Although adsorption data could not be found for SSZ-13 zeolite, the single-gas permeances indicate that CO_2 adsorbs more strongly than the other gases and thus permeates faster at 298 K. Silicalite,[41] A- and X-type,[42] SAPO-34,[10] and mineral chabazite[42] adsorb CO_2 more strongly than other light gases so it is reasonable that SSZ-13 behaves in a similar manner. The SSZ-13 membranes, except M1, permeated CH_4 faster than N_2 at 473 K, indicating that the membranes adsorb CH_4 more strongly than N_2, because N_2 is expected to diffuse through SSZ-13 pores faster than CH_4 because of its smaller kinetic diameter.

The permeances of all gases except CO_2 increased with temperature because their diffusivities increased. The coverages of all gases are expected to be lower at 473 than 298 K because adsorption is exothermic; the CO_2 coverage might have decreased significantly, and the increase in its diffusivity did not compensate for its decrease in coverage. Thus, the CO_2 permeance was lower at 473 K than at 298 K. Note that $i\text{-}C_4H_{10}$ permeated faster than $n\text{-}C_4H_{10}$ even though $i\text{-}C_4H_{10}$ is larger. Both of these molecules diffuse through nonzeolite pores. Similar behavior has been reported for MFI membranes.[43−46]

(41) Bakker, W. J. W.; van den Broeke, L. J. P.; Kaptijn, F.; Moulijn, J. A. *AIChE J.* **1997**, *43*, 2203.
(42) Breck, D. W. *Zeolites Molecular Sieves, Structure, Chemistry and Use*; John Wiley and Sons: New York, 1971; p 654.
(43) Bai, C.; Jia, M. D.; Falconer, J. L.; Noble, R. D. *J. Membr. Sci.* **1995**, *105*, 79.
(44) Coronas, J.; Falconer, J. L.; Noble, R. D. *AIChE J.* **1997**, *43*, 1797.

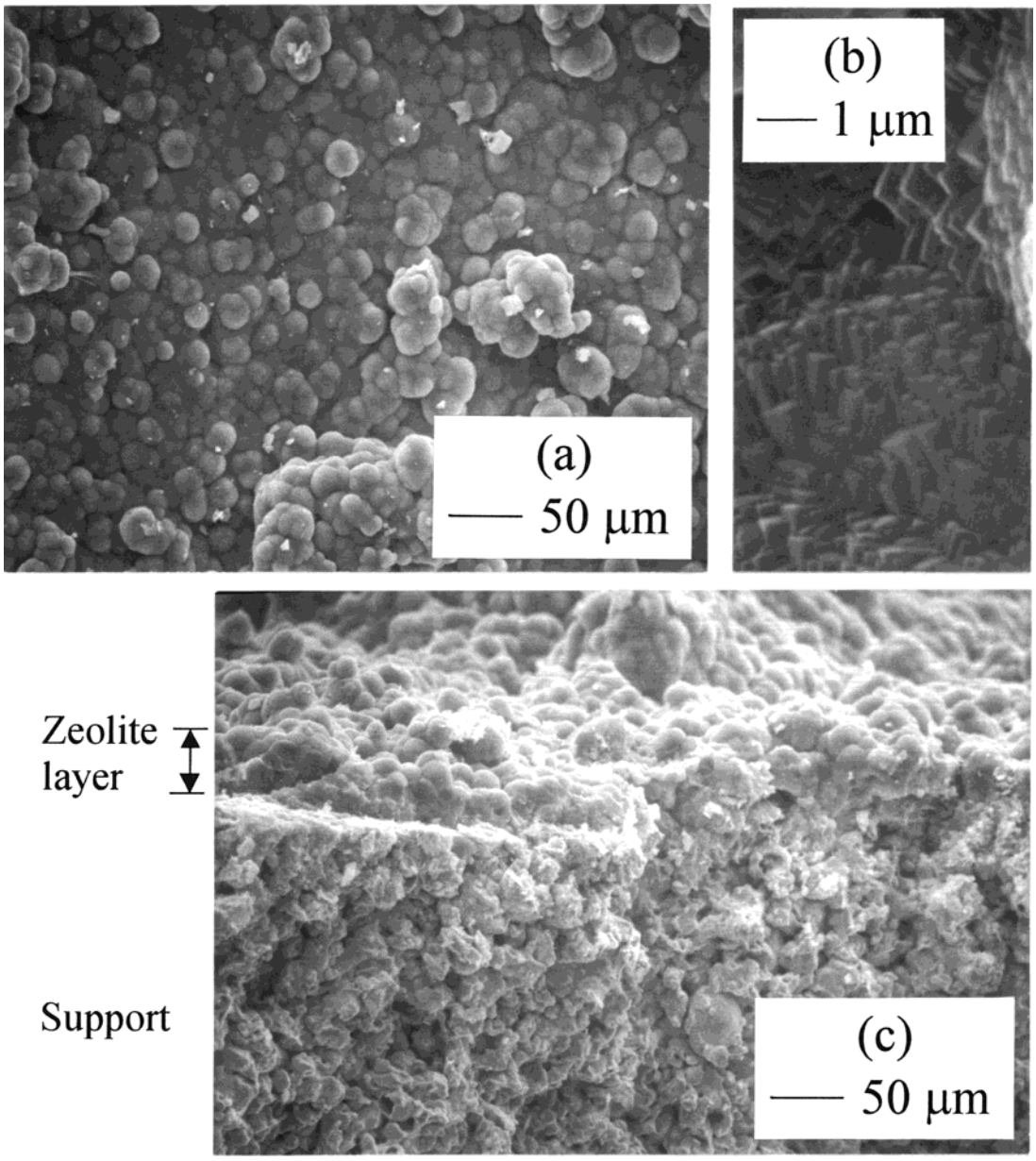

Figure 2. SEM images of a SSZ-13 membrane (M6) on a porous stainless steel tube: (a,b) surface, and (c) cross section.

Separation of Light-Gas Mixtures. Binary mixtures of H_2, CO_2, N_2, and CH_4 were separated with membrane M1 because it had the highest ideal selectivities. Figures 5 and 6 show the separation results for CO_2/CH_4 and CO_2/N_2 mixtures, respectively. The CO_2 permeances decreased, but the N_2 and CH_4 permeances increased with increasing temperature. The single-gas and mixture permeances differed at low temperatures, but they were almost the same above approximately 400 K. The ideal and separation selectivities, which decreased with temperature similarly to the CO_2 permeances, were practically the same except at 298 K. The highest CO_2/CH_4 and CO_2/N_2 separation selectivities at 298 K were 13 and 11, respectively.

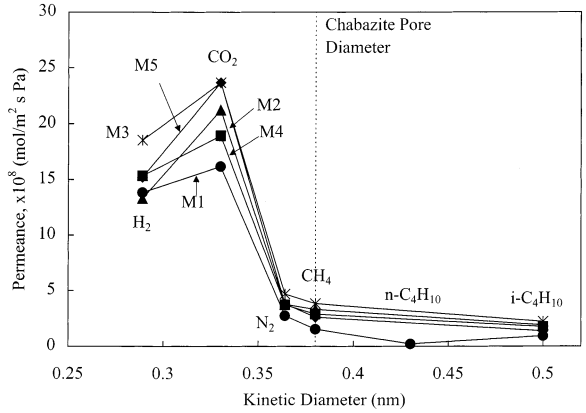

Figure 3. Single-gas permeances through SSZ-13 membranes at 298 K as a function of kinetic diameter.

Figure 7 shows the single-gas and separation results for H_2/CH_4 mixtures. The single-gas H_2 permeances had a minimum around 370 K, but the mixture permeances increased with temperature. The single-gas H_2 per-

(45) Tsapatsis, M. In *Proceedings of the International Workshop on Zeolitic Membranes and Films*, Japan Association of Zeolite, The Membrane Society of Japan, and Japan Fine Ceramics Center, Gifu, Japan, 1998; p 37.

(46) Hedlund, J.; Noack, M.; Kolsch, P.; Creaser, D.; Caro, J.; Sterte, J. *J. Membr. Sci.* **1999**, *159*, 263.

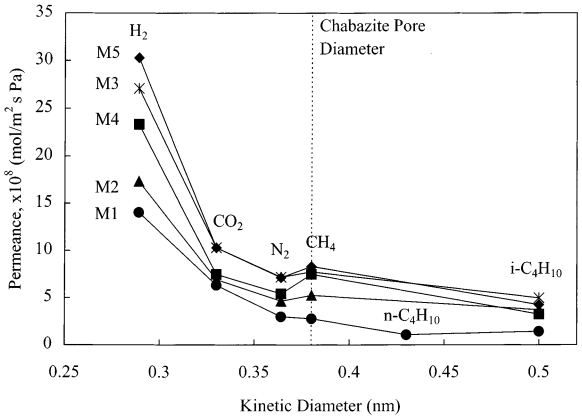

Figure 4. Single-gas permeances through SSZ-13 membranes at 473 K as a function of kinetic diameter.

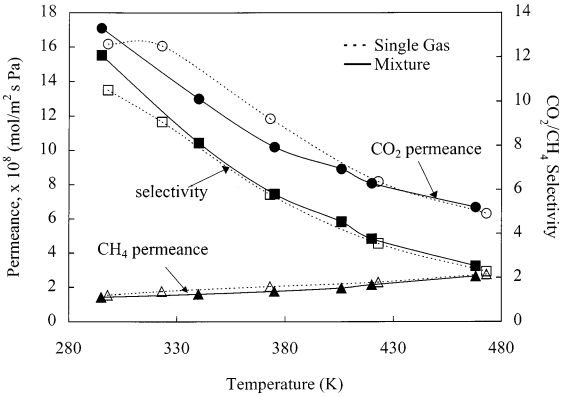

Figure 5. Single-gas and mixture permeances and ideal and separation selectivities of a 50/50 CO_2/CH_4 mixture as a function of temperature for membrane M1.

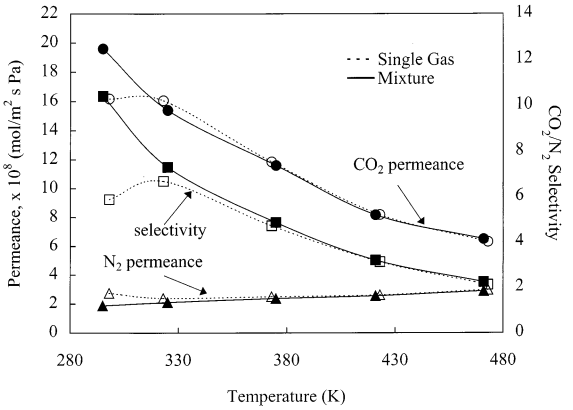

Figure 6. Single-gas and mixture permeances and ideal and separation selectivities of a 50/50 CO_2/N_2 mixture as a function of temperature for membrane M1.

meances were significantly higher than the mixture H_2 permeances below approximately 370 K, and they were almost equal above 370 K. The CH_4 permeance behaved the same in the H_2/CH_4 mixture as in the CO_2/CH_4 mixture, increasing continuously with temperature. The ideal selectivity decreased with temperature, and this decrease was more appreciable at low temperatures. The separation selectivity had a maximum of 7.7 around 373 K.

The differences between ideal and separation selectivities are attributed to preferential adsorption. Bakker et al.[47] showed that a strongly adsorbed molecule can hinder the transport of a weakly adsorbed molecule. In the separations of CO_2/CH_4 (Figure 5), CO_2/N_2 (Figure 6), and H_2/CH_4 (Figure 7), the mixture permeances and separation selectivities deviated from the single-gas permeances and ideal selectivities at low temperatures because the slower-permeating molecule inhibits transport of the faster-permeating molecule. The effect of inhibition increased as the adsorption strength of the slower-permeating molecule increased and that of the faster-permeating molecule decreased. Therefore, the deviation from the single-gas permeances was small for the CO_2/N_2 mixture, but it was large for the H_2/CH_4 mixture.

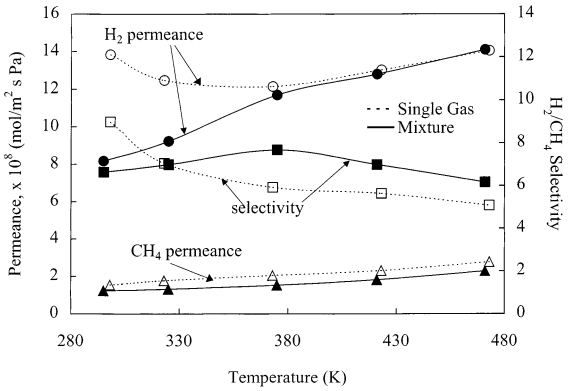

Figure 7. Single-gas and mixture permeances and ideal and separation selectivities of a 50/50 H_2/CH_4 mixture as a function of temperature for membrane M1.

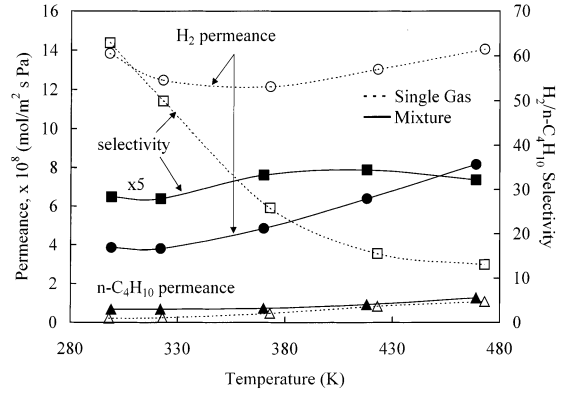

Figure 8. Single-gas and mixture permeances and ideal and separation selectivities of a 50/50 H_2/n-C_4H_{10} mixture as a function of temperature for membrane M1.

As the temperature increased, the mixture permeances and selectivities for light gases approached the single-gas permeances and selectivities. Adsorption coverages were expected to be lower at high temperatures, and the membrane separated molecules by differences in diffusivities at high temperatures. The selectivities and permeances reflected the expected order of diffusivities at 473 K: $H_2 > CO_2 > N_2 > CH_4$.

The membrane separated a 50/50 H_2/n-C_4H_{10} mixture, as shown in Figure 8. The H_2 and n-C_4H_{10} permeances exhibited similar trends in mixtures and as single gases. The H_2 mixture permeance, however, was approximately 30% of its single-gas permeance at 298 K and

(47) Bakker, W. J. W.; Kapteijn, F.; Poppe, J.; Moulijn, J. A. *J. Membr. Sci.* **1996**, *117*, 57.

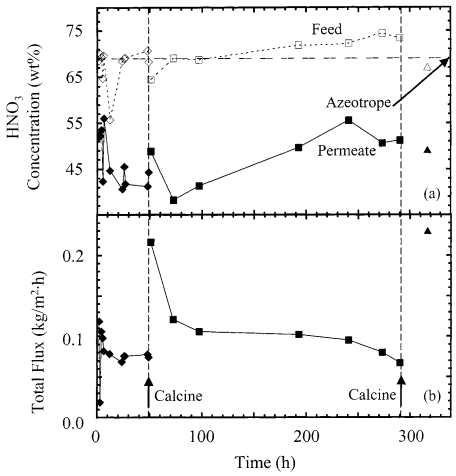

Figure 9. Transient measurements of (a) feed and permeate HNO_3 concentrations and (b) total fluxes through membrane M5 at 298 K. A 69.5 wt % HNO_3 feed solution was used, and the separation was interrupted after 50 and 300 h to calcine the membrane. The membrane was removed from the system and calcined at the indicated times.

Table 3. Steady-State H_2O/HNO_3 Separation Factors and Total Fluxes through SSZ-13 Membranes Using a 69.5 wt % HNO_3 Feed at 298 K

membrane	% HNO_3 in permeate	H_2O/HNO_3 separation factor	total flux ($kg/m^2 \cdot h$)
M5	40.6	3.3	0.07
M7	41.9	3.2	0.04

60% at 473 K, showing that the *n*-C_4H_{10} inhibited H_2 permeation. Because *n*-C_4H_{10} cannot enter the zeolite pores, the inhibition occurs in nonzeolite pores. Pores in series with the zeolite pores could adsorb *n*-C_4H_{10} and inhibit H_2 permeation, so we cannot estimate the fraction of H_2 permeating through nonzeolite pores.

The increase of H_2 permeance with temperature was mainly due to the increased mobility of H_2; the *n*-C_4H_{10} inhibited H_2 less at higher temperature, but the *n*-C_4H_{10} permeance also increased with temperature, so the separation selectivity did not change much. The separation selectivities showed a weak maximum of approximately 6.9 at 420 K.

Separation of HNO_3/H_2O Solutions. As shown in Table 3, the SSZ-13 membranes effectively removed water from 69.5 wt % aqueous HNO_3 at 298 K. The membranes broke the azeotrope, and the permeate concentration was approximately 40 wt % HNO_3.

The stability of membrane M5 in strong acid was measured by separating 69.5 wt % HNO_3 solution for 13 days at 298 K. During this period, the pervaporation was interrupted after 50 and 300 h to calcine the membrane at 623 K (Figure 9). After 50 h, the total flux was 0.07 $kg/m^2 \cdot h$ with a permeate concentration of 41 wt % HNO_3, which corresponds to a separation factor of 3.3. After calcination, the permeate concentration was initially 49 wt % and decreased to 41 wt % HNO_3 within 50 h. The dashed lines in Figure 9 indicate the starting time of the next pervaporation run after calcination. Although the permeate concentrations before and after calcination were reproducible, the total flux was higher after calcination. The permeate and feed concentrations slowly increased, and the total flux decreased between 100 and 290 h. After 290 h, the feed and permeate concentrations were 73 and 51 wt %, respectively. Degradation of the membrane by HNO_3 probably caused the increased permeate concentration, but the total flux decreased with time, which would not be expected for a membrane with increasing nonzeolite pores caused by degradation. This suggests that impurities in the feed might have adsorbed in the membrane pores. Approximately 26 h after the second calcination, the total flux was significantly higher, and the separation factor was lower than at the same time after the first calcination.

Another membrane (M7) was exposed to boiling 69.5 wt % HNO_3 and no longer separated H_2O from HNO_3. The Si/Al ratio in the membrane was 13.3 (EDX), which is close to the expected ratio of 14, and the XRD pattern was identical to that shown in Figure 1b, indicating that the SSZ-13 framework was not destroyed by the acid. This conclusion is also supported by measurements of the stability of SSZ-13 powder in 69.5 wt % HNO_3 at room temperature. These measurements showed that 5% of the initial Al in the zeolite dissolved in 3 days, but no more dissolved during 2 additional days. The amounts of Si in the acid after 3 and 5 days were near the detection limit of the ICP-AES. The negligible amount of Si dissolved implies that the zeolite structure does not collapse even though acid leached Al from the framework. The HNO_3 might increase the nonzeolite pore size by attacking the intracrystalline boundaries or by corroding the support. Although no color was observed in the permeate solution, the feed solution turned slightly yellow after long-term pervaporation. This membrane was prepared in the Na^+ form, but EDX line analysis showed that the average Al/Na ratio in the membrane after 9 h of pervaporation was 300 with almost no Na remaining, indicating that Na^+ exchanged with H^+ during pervaporation. The membrane was still selective, however, even though the Na was removed.

The temperature dependence of water/HNO_3 separation was also investigated. Pervaporation measurements using 69.5 wt % HNO_3 at 323 K showed that the separation factor and total flux increased with temperature for membrane M5. After the transient measurements, the membrane had a total flux of 0.52 $kg/m^2 \cdot h$ at 323 K and a separation factor of 2.5, which corresponds to 48.1 wt % HNO_3 in the permeate. The flux increased from 0.13 $kg/m^2 \cdot h$ at 298 K to 0.77 $kg/m^2 \cdot h$ at 323 K for membrane M8, and the HNO_3 permeate concentration decreased from 64.6 wt % at 298 K to 53.9 wt % at 323 K using a 69.5 wt % HNO_3 feed. High temperatures improved the membrane performance, but the membrane stability in acid is probably greater at low temperatures.

Although the SSZ-13 membranes prepared in this study contain nonzeolite pores, the membranes broke the HNO_3/water azeotrope. Nitric acid at high concentrations appears to slowly decompose SSZ-13. A chabazite structure membrane with a higher Si/Al ratio would be more resistant to HNO_3.

Summary

Membranes of small-pore zeolite SSZ-13 (0.38-nm pore diameter) were synthesized on tubular stainless steel supports. These membranes separated light-gas mixtures of CO_2/N_2, CO_2/CH_4, H_2/CH_4, and H_2/n-C_4H_{10}

with selectivities higher than the Knudsen selectivities and removed water from nitric acid to break the azeotrope at 69.5 wt % HNO_3 even though they contained nonzeolitic pores. The membranes showed short-term stability under low-pH conditions.

Acknowledgment. We gratefully acknowledge support by the NSF I/U CR Center for Membrane Applied Science and Technology (MAST). We thank Dr. William L. Schinski of Chevron Research & Technology Co. for his valuable suggestions on the preparation of TMAdaOH and Ian Carbone for experimental assistance. We are grateful to Pall Corp. for providing the stainless steel supports. The authors also acknowledge support by TUBITAK-NATO (H.K.) and a fellowship from the U.S. Department of Education Graduate Assistantships in Areas of National Need (GAANN) Program (T.C.B.).

CM020248I